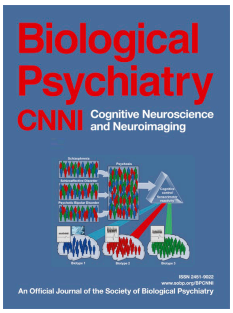

The Topography of Striatal Dopamine and Symptoms in Psychosis: An Integrative PET and MRI study

Robert A. McCutcheon, Sameer Jauhar, Fiona Pepper, Matthew M. Nour, Maria Rogdaki, Mattia Veronese, Federico E. Turkheimer, Alice Egerton, Philip McGuire, Mitul M. Mehta, Oliver D. Howes

PII: S2451-9022(20)30097-5

DOI: https://doi.org/10.1016/j.bpsc.2020.04.004

Reference: BPSC 581

To appear in: *Biological Psychiatry: Cognitive Neuroscience and Neuroimaging*

Received Date: 13 December 2019

Revised Date: 10 April 2020

Accepted Date: 10 April 2020

Please cite this article as: McCutcheon R.A, Jauhar S., Pepper F., Nour M.M, Rogdaki M., Veronese M., Turkheimer F.E, Egerton A., McGuire P., Mehta M.M. & Howes O.D, The Topography of Striatal Dopamine and Symptoms in Psychosis: An Integrative PET and MRI study *Biological Psychiatry: Cognitive Neuroscience and Neuroimaging* (2020), doi: https://doi.org/10.1016/j.bpsc.2020.04.004.

The Topography of Striatal Dopamine and Symptoms in Psychosis: An Integrative PET and MRI study

Robert A McCutcheon*[a,b,c]

Sameer Jauhar* [a,b,c]

Fiona Pepper[d]

Matthew M Nour[a,e,f]

Maria Rogdaki[a,b,c]

Mattia Veronese[d]

Federico E Turkheimer[d]

Alice Egerton[a]

Philip McGuire[a]

Mitul M. Mehta[d]

Oliver D Howes[a,b,c]

[a]Department of Psychosis Studies, Institute of Psychiatry, Psychology & Neuroscience, Kings College London, De Crespigny Park, London SE5 8AF, UK

[b]Psychiatric Imaging Group, MRC London Institute of Medical Sciences, Hammersmith Hospital, London, W12 0NN, UK

[c]Institute of Clinical Sciences, Faculty of Medicine, Imperial College London, London, W12 0NN, UK

[d]Department of Neuroimaging, Institute of Psychiatry, Psychology & Neuroscience, Kings College London, De Crespigny Park, London SE5 8AF, UK

[e]Max Planck UCL Centre for Computational Psychiatry and Ageing Research, 10-12 Russell Square, London, WC1B 5EH, UK

[f]Wellcome Centre for Human Neuroimaging (WCHN), University College London, London, United Kingdom

*These authors contributed equally to the manuscript

Running title: Dopamine and Psychotic Symptoms

Keywords: schizophrenia; striatum; resting state; functional connectivity; positive symptoms; negative symptoms

Abstract

Background

Striatal dopamine dysfunction is thought to underlie symptoms in psychosis, yet it remains unclear how a single neurotransmitter could cause the diverse presentations that are observed clinically. One hypothesis is that the consequences of aberrant dopamine signalling vary depending on where within the striatum the dysfunction occurs. Positron emission tomography (PET) allows for the quantification of dopamine function across the striatum. In the current study we use a novel method to investigate the relationship between spatial variability in dopamine synthesis capacity and psychotic symptoms.

Methods

We used a multimodal imaging approach combining ^{18}F-DOPA PET and resting state MRI in 29 patients with first episode psychosis and 21 healthy controls. In each participant, resting state functional connectivity maps were used to quantify the functional connectivity of each striatal voxel to well-established cortical networks. Network-specific striatal dopamine synthesis capacity(Ki^{cer}) was then calculated for the resulting connectivity defined parcellations.

Results

The connectivity defined parcellations generated Ki^{cer} values with equivalent reliability, and significantly greater orthogonality to standard anatomical parcellation methods. As a result, dopamine-symptom associations were significantly different from one another for different subdivisions, whereas no unique subdivision relationships were found when using an anatomical parcellation. In particular, dopamine function within striatal areas connected to the default mode network was strongly associated with negative symptoms($p<0.001$).

Conclusion

These findings suggest that individual differences in the topography of dopamine dysfunction within the striatum contribute to shaping psychotic symptomatology. Further validation of the novel approach in future studies is necessary.

Introduction

Psychotic symptoms occur across a range of mental disorders including schizophrenia, bipolar disorder, and depression. Even within a single disorder such as schizophrenia, marked symptomatic diversity exists, with clusters including positive symptoms such as hallucinations and delusions, negative symptoms such as social withdrawal and amotivation, affective symptoms and cognitive deficits (1–5). Given that both symptoms and neurobiological abnormalities cross diagnostic boundaries (6), there has been an increasing focus on characterising neuronal circuits that have transdiagnostic relevance for understanding psychopathology (7, 8). Aberrant striatal dopamine signalling, and in particular, increased presynaptic dopamine synthesis capacity, has been linked to psychotic symptoms (9–13). Although most work has focused on the link with positive symptoms (10–12, 14), it remains an open question as to whether striatal dopamine alterations are linked to other symptoms seen in psychotic disorders, such as cognitive and negative symptoms (15–17).

The striatum is a central processing hub, receiving input from almost the entire cortex (18), and plays a role in sensory, motor, cognitive, and affective processes (19–21). Thus, dysfunction in the striatum could plausibly lead to a range of heterogeneous symptoms observed in psychotic disorders. Cortical neurons largely project to discrete regions within the striatum (22), and cortical topography is mirrored striatally(18). Dopamine is a neuromodulator that plays a key role in regulating inputs and signal transmission from the striatum(23). Given this preserved topographical mapping of cortical inputs, the precise location of dopamine dysfunction within the striatum is likely to determine which particular corticostriatal circuits are affected (9), and in turn may be expected to shape symptomatology.

Improvements in the resolution of PET scanners have meant that greater spatial precision is possible when imaging striatal dopamine. This has led to the finding that dopamine dysfunction in schizophrenia is not uniform across the striatum, but shows significant spatial variability (9, 24–26). When investigating dopamine function with typical anatomically-based parcellation methods, however, a high degree of correlation is observed between striatal subdivisions (26). This collinearity precludes investigation of the hypothesis that spatial variability may shape symptomatology(26).

Resting state functional magnetic resonance imaging (rs-fMRI) can be used to quantify the functional connectivity between two brain regions or voxels, by quantifying the correlation between the neural activity timeseries within each region (27, 28). This allows one to map individualised corticostriatal functional connectivity, and generate connectivity defined striatal parcellations. Striatal parcellations derived from participant-specific corticostriatal connectivity patterns may better capture the functional topography of the striatum compared to standard group level anatomically based striatal parcellations. When combined with PET imaging, this method may lead to greater orthogonality between dopamine measures within striatal subdivisions compared to anatomically based methods, and thereby allow testing of the hypothesis that spatial variation in dopamine function across the striatum influences symptomatology.

In the present study, we use rs-fMRI to map functional corticostriatal connections in patients presenting with first episode psychosis, and PET to examine striatal dopamine synthesis capacity within the same individuals. By combining rs-fMRI and PET we were able to evaluate dopamine function within subdivisions of the striatum that had been defined on the basis of their cortical connectivity at an individual level. We first validate this method by comparing with typical anatomically based methods of parcellating the striatum in terms of test-retest reliability and subdivision orthogonality(29, 30). We next used this method to examine whether dopamine synthesis capacity within individualised connectivity-defined regions correlated with Marder Factor scores (factor analysis derived subscales of the Positive and Negative Syndrome Scale (PANSS)) (3) and investigate whether relationships between dopamine-symptom associations are significantly different between subdivisions .

Materials and methods

Overview

29 first episode psychosis patients and 21 healthy controls received a 3,4-dihydroxy-6-[18F]fluoro-L-phenylalanine (^{18}F-DOPA) PET scan and an MRI scan. Clinical ratings were performed using the Positive and Negative Syndrome Scale (PANSS) by a consultant psychiatrist, blind to imaging outcome measures. For each participant, we used functional connectivity between cortical resting state networks and the striatum to generate individualised connectivity-defined striatal parcellations. We then combined this with PET data to calculate the dopamine synthesis capacity (Ki^{cer}) for these connectivity defined parcels. We next combined test-retest datasets for both ^{18}F-DOPA and resting state MRI(31, 32), to compare the reliability and collinearity of Ki^{cer} values calculated using this method, with those calculated using a traditional anatomically based parcellation. We then investigated whether dopamine function within these connectivity-defined striatal subdivisions showed a relationship with symptomatology in patients, and evaluated the specificity and statistical significance of any observed relationships using a permutation testing approach. The analysis approach is summarised in Figure 1 and described in detail in the Supplement.

Participants

Participants were experiencing a first episode of psychotic illness, meeting ICD-10 criteria (33), and were either antipsychotic naïve (n=11), antipsychotic free for at least 6 weeks (n=16), or minimally treated for less than 2 weeks (n=2). Age-matched (within 5 years) healthy controls were recruited from the same geographical area through local media advertisements. Controls had no previous or current history of psychiatric illness (assessed by the Structured Clinical Interview for DSM-IV Axis I disorders), no concurrent psychotropic medication use, and no family history of psychosis. See Supplementary Methods and previously published reports for further details regarding recruitment and assessment (34, 35). Some of the data for these participants has been previously reported (14, 34–36).

Image Acquisition

Participants received an ^{18}F-DOPA pet scan, providing a measure of striatal dopamine synthesis capacity (37). The cerebellum was used as a reference region, and voxelwise parametric images of Ki^{cer} were constructed from movement-corrected images using a wavelet-based Patlak approach (see Figure S1) (38). We also determined Ki^{cer} for limbic, associative (the pre- and postcommissural caudate, and precommissural putamen), and sensorimotor (post-commisural putamen) striatal subdivisions, using the anatomically defined approach outlined by Martinez et al. (30). Participants also received an 8.5-minute rfMRI scan on a 3T GE Signa MR scanner. See Supplemental Methods for further details.

Image Analysis: Cortical Network Definition

fMRI signal time series were extracted from the 333 cortical regions (nodes) of the Gordon cortical atlas (a network parcellation based on fMRI functional connectivity patterns observed in a sample of 120 healthy young adults). Functional connectivity between every pair of nodes was defined as the pairwise z-transformed Pearson correlation coefficients between the fMRI timeseries of each region (39), and was used to define a 333*333

functional connectivity matrix for each participant. The Louvain community detection algorithm was then employed on this whole-cortex connectivity matrix, to group each cortical node into non-overlapping communities in a manner that maximises the modularity of the final network (40). The detected communities corresponded to well recognised resting state networks: the default mode (DMN), sensorimotor (SMN), cinguloopercular (CON), dorsal attention (DAT), auditory (AUD) and visual (VIS) networks (Figure S2). The visual network, was excluded from subsequent analyses given its relative lack of direct connections with the striatum (41). Analysis was performed with in-house Python code.

Image Analysis: Striatal Parcellation and PET Integration

An individualised probabilistic approach was employed. For each participant, for each cortical network identified above, each striatal voxel was assigned a connectivity score between 0 and 1 based on its mean connectivity to all nodes within that network (see Figure S3). A weighted striatal map was thereby constructed for each of the networks identified. We used a probabilistic (as opposed to a winner-takes-all) approach given the fact that although corticostriatal pathways run in parallel there is a high degree of overlap (18). These striatal maps were then overlaid on the PET voxelwise Ki^{cer} maps to enable the calculation of network-specific Ki^{cer} values.

Image Analysis: Reliability and Orthogonality

16 (8 participants) test-retest PET maps were available from a previous study (31). These were paired with 80 (40 participants) test-retest resting state scans from the Human Connectome Project (HCP) (32). Using the methods described above, individual connectivity defined Ki^{cer}s were calculated for each PET-resting state pair. This provided five test-retest datasets where each set contains the same 8 PET participants, but different, non-overlapping HCP participants. For each PET participant, Ki^{cer} values were also calculated using the widely-used anatomically defined Martinez striatal parcellation(30). Intraclass correlation coefficients (ICC) between test and retest scans were calculated using the R package 'irr' 0.84.1(42). We employed the same method used in the original study of ^{18}F-DOPA test-retest reliability using the method of Shrout and Fleiss with two way random subject effects, fixed session effects, and parcel Ki^{cer}s considered the average of individual voxels (31, 43). The ideal method for assessing reliability would involve PET and MRI scans obtained from the same individuals, as the fact that the PET and MRI scans are from different individuals has the potential to reduce the reliability of the method. As such this analysis provides a lower bound on the method used for calculating subdivision specific Ki^{cer} values. We also performed an analysis of solely the MRI data for the same 80 HCP scans, in which we investigated test-retest reliability of mean connectivity strength for each striatal subdivision (i.e. the reliability of the weighting that is subsequently used to calculate the Ki^{cer} values).

Using data from the current study, we investigated whether the connectivity defined subdivisions showed greater orthogonality in terms of Ki^{cer} values compared to anatomically defined subdivision Ki^{cer}s. Specifically, the correlation coefficients between subdivisions across all participants defined with one method were compared to the correlation coefficients between subdivisions defined using the other method, using a the method of Silver et al. implemented in the R package *cocor* (version 1.1-3) (44).

Image Analysis: Dopamine-Symptom Relationships

Based on previous findings (13, 34, 45), we tested the hypothesis that Ki^{cer} would be linearly related to severity of symptoms. Symptoms were grouped according to the Marder five factor model(3), and Pearson correlation coefficients were calculated between each factor and each network-specific Ki^{cer}.

Statistical significance was assessed using two separate permutation testing approaches – participant level permutations, and cortical node permutations. A permutation testing approach was employed as this is non-parametric and makes minimal assumptions regarding the structure of the data. In both approaches the relationship between all five Marder factors and the five connectivity parcellation defined Ki^{cer}s were tested, and false discovery rate (FDR) correction for the 25 tests undertaken was performed (46). The first approach involved permuting at the participant level (i.e. shuffling the mapping between participant-specific symptom scores and Ki^{cer} values), generating a null distribution by calculating correlation coefficients after permuting Ki^{cer} values while keeping symptom scores fixed (10,000 permutations). We then tested statistical significance by comparing the correlation coefficients between subdivision Ki^{cer} and symptom scores observed in the actual data, with the coefficients observed in the permuted data.

The participant level approach, however, does not account for the general relationship between whole striatum Ki^{cer} and total symptoms, in that any significant findings could reflect a general association between whole striatal Ki^{cer} and symptoms in general, rather than a relationship between a symptom domain and a Ki^{cer} from a specific connectivity defined parcellation. Therefore, we also employed a separate approach in which we permuted the cortical nodes assigned to networks (10,000 permutations), thereby creating a null distribution that retained the relationship with mean striatal dopamine synthesis capacity (Figure 1B). With this approach we were able to test whether an observed subdivision Ki^{cer}-symptom correlation was truly specific to that identified subdivision over and above the general striatal Ki^{cer}-symptom relationships present in the data. The use of both permutation approaches therefore represents a particularly robust analysis of the statistical significance of our observed dopamine-symptoms correlations; accounting for outliers, skewed data distributions, and allowing for testing of the specificity of the subdivision-symptom relationships.

An aim of the current study was to determine whether the connectivity-based approach had the ability to highlight dopamine-symptom relationships that were distinct between subdivisions. We therefore tested whether symptom-dopamine associations were significantly different between subdivisions. For a given symptom domain, for each possible pair of subdivisions, we calculated the true absolute difference between subdivision-symptom correlation coefficients. We then determined statistical significance by comparing this true difference with the equivalent differences observed in the (participant level) permuted data.

Image Analysis: Patient-Control Differences in Connectivity and Dopamine Function

We also tested for differences in striato-cortical connectivity between patients and controls, as this could potentially lead to differences in the connectivity-based parcellations. We first investigated whether differences existed in subdivision weightings. For each individual, for each connectivity defined subdivision, we calculated

the mean of all the connectivity values within that subdivision. We then compared these values between patients and controls using an independent samples t-test.

In addition to differences in overall weightings there also exists the possibility that patients and controls may differ in terms of the spatial layout of the connectivity-based subdivisions. In order to investigate this, for each subdivision we tested whether there was a difference in weightings for patients compared to controls in either of the three axes (x, y, z). For the x-axis, for example, this involved multiplying each subject's 3 dimensional connectivity-based subdivision by a 3 dimensional matrix that showed a linear progression in value only across the x-axis , we then summed the values for that individual's newly weighted subdivision, and used this value in an independent sample t-test between patients and controls, allowing us to see whether patients or controls showed a tendency to show greater laterality along the x-axis in terms of this subdivision's weighting (see Figure S4).

We also examined patient-control differences in Ki^{cer} for each striatal subdivision using an independent samples t-test. 19 of the patients and 12 of the controls were included in a previously reported study(34), in which raised dopamine synthesis capacity was present only in responders to antipsychotic treatment, we therefore also investigated patient control Ki^{cer} differences after only including patients subsequently determined to be antipsychotic responders (n=11).

Data availability

Code used for analysis is freely available at https://github.com/robmcc10/ dopamine_symptoms_bp_cnni. Data is available from the authors upon request.

Results

Participants

50 participants took part in the study (21 controls and 29 patients). Demographic details are given in Table 1. Mean total PANSS score for patients was 66.7 (SD 20.7).

Cortical Network Assignment and Striatal Connectivity Maps

The community detection algorithm assigned nodes to 5 separate networks, these corresponded to well recognised resting state networks (DMN, AUD, DAT, SMN, CON, see Figure S2). The connectivity between these networks and the striatum was calculated at the individual participant level, although for display purposes group averaged maps are shown in Figure 2.

Reliability and Comparison with Existing Parcellation Methods

When examining reliability and orthogonality we compared our individualised connectivity-based approach to an anatomical approach (29, 30). Reliability using both methods was good, but the ICC was generally higher using the connectivity-based approach where it ranged from 0.73-0.78, compared to 0.65-0.80 for the anatomically defined subdivisions (see supplementary results). ICC values of solely the rs-fMRI based connectivity parcellations was fair to good for all subdivision (0.48-0.65) except DAT (ICC=0.32) (see supplementary results) (47).

In addition to reliability, orthogonality between subdivision Ki^{cer}s is required for the investigation of unique subdivision-symptom relationships, as a high degree of correlation between subdivisions effectively precludes the identification of relationships specific to a subdivision. Correlations between subdivision Ki^{cer}s demonstrated that the anatomical subdivisions showed highly collinear relationships (r_p=0.76-0.92), while in contrast the connectivity defined subdivisions showed much greater orthogonality (r_p 0.23-0.65). The connectivity-based approach showed numerically greater orthogonality for all 30 possible comparisons between the methods, which was statistically significant for 25 of these (Figure 3).

Symptom-Dopamine Relationships

The associations between Marder Factor scores and subdivision Ki^{cer}s are displayed in Figure 4. When permuting participants (Figure 4A) significant positive associations were observed between AUD Ki^{cer} and the Disorganisation factor (r=0.40, p=0.01, FDR p=0.11), and between CON Ki^{cer} and the Depression/Anxiety factor (r_p=0.37, p=0.028, FDR p=0.11). DMN Ki^{cer} showed a significant association with all factors (Depression/Anxiety r_p=0.47, p= 0.003, FDR p=0.04; Disorganisation r_p=0.38, p=0.02, FDR p= 0.11; Excitement r_p=0.33, p=0.03, FDR p=0.11 ; Negative r_p=0.49, p=0.0009, FDR p=0.02 ; Positive r_p=0.37 , p= 0.025, FDR p=0.11) (see. Figure 4B).

In terms of the anatomically defined regions the whole striatum showed significant associations with Depression/ Anxiety (r_p=0.53 , p=0.002 , FDR p= 0.02), Excitement (r_p=0.43, p= 0.01, FDR p=0.048), and Positive (r_p=0.32 , p=0.048, FDR p=0.09) factors. The three subdivisions were all significantly associated with Depression/Anxiety and Excitement factors. The associative subdivision showed the strongest relationship

(Depression/Anxiety r_p= 0.53, p= 0.002, FDR p= 0.02; Excitement r_p=0.42, p= 0.01, FDR p=0.048), followed by the Sensorimotor subdivision (Depression/Anxiety r_p= 0.48, p= 0.006, FDR p= 0.04; Excitement r_p= 0.40, p=0.02, FDR p=0.07), and the limbic subdivision (Depression/Anxiety r_p= 0.35, p= 0.03, FDR p= 0.08; Excitement r_p= 0.35, p= 0.03, FDR p=0.08). Symptom-subdivision relationships remained statistically significant in a sensitivity analysis excluding the two minimally treated participants (Figure S5), and also when visual network nodes were included (Figure S6).

As discussed above, permuting participants does not account for a more general overall striatal Ki^{cer}-symptom association. When using the cortical node permutation approach DMN Ki^{cer} still showed significant associations, those being with Negative (p=0.0015, FDR p=0.038) Depression/Anxiety (p=0.023, FDR p =0.19), and Disorganization (p=0.034, FDR p=0.21) factors. AUD Ki^{cer} also show an association with the Disorganisation factor (p=0.022, FDR p=0.19) (Figure S7).

As shown above, the connectivity-based approach led to significantly greater orthogonality between subdivisions compared to the anatomical parcellation. We examined whether this was accompanied by symptom-subdivision relationships that were significantly different from one another (Figure 4C). For Depression/Anxiety and Excitement Marder factors the connectivity defined SMN subdivision showed a significantly lower correlation coefficient compared to the whole striatum (Depression/Anxiety p=0.04, Excitement p=0.04) and associative striatum (Depression/Anxiety p=0.03; Excitement p=0.04). For the Disorganisation factor the CON subdivision showed a significantly lower coefficient compared to the DMN (p=0.03) and AUD (p=0.04) subdivisions. For the Negative factor the DMN subdivision showed a greater coefficient than either the DAT (p=0.005) or CON (p=0.04) subdivisions. For the Positive factor the DMN subdivision showed a greater coefficient than either DAT (p=0.05) or CON (p=0.02) subdivisions, and the DAT subdivision showed a lower coefficient compared to associative subdivision (p=.04) and whole striatum (p=0.05). It is of note that for no symptom-subdivision relationship did any of the anatomical subdivisions differ significantly from one another.

Patient-Control Differences in Striato-Cortical Connectivity and Ki^{cer}

When investigating differences between groups in terms of striatal connectivity differences, no significant differences were found between groups in terms of the mean connectivity for any of the defined subdivisions (p>0.3 for all subdivisions, Figure S8). There were also no differences between patients and controls in terms of subdivision spatial distribution of connectivity (p>0.3 for all comparisons, see supplementary materials).

Differences between patients and controls in terms of Ki^{cer} were also examined. No statistically significant differences were observed between patients and controls for any subdivision (Figure S9). In a post-hoc analysis based on findings in an overlapping cohort that raised dopamine synthesis capacity is present only in responders to antipsychotic treatment (34), we restricted the analysis to those characterised as antipsychotic responder (n=11). In this subgroup dopamine synthesis capacity was higher compared to controls for the DMN (t=2.78, p=0.009) and DAT (t=2.31, p=0.028) Ki^{cer} (see Table 2).

Discussion

In the current study we describe a novel method for integrating rs-fMRI and ^{18}F-DOPA PET in order to derive measures of dopamine function from connectivity defined striatal subdivisions. The indices of dopamine function calculated using these connectivity defined subdivisions demonstrated good reliability, and also show significantly greater orthogonality compared to anatomical defined subdivisions. Using this approach, we found a strong positive association between the severity of negative symptoms and dopamine synthesis capacity within regions of the striatum functionally linked to the default mode network.

While previous studies have investigated the relationship between striatal dopamine function and symptoms in psychotic disorders, this has predominantly been at the level of the whole striatum, and so has not addressed the question of subdivision specific relationships (13, 34, 45). Although more recent studies have examined subdivisions, the typical approach employed precludes investigation of the current hypothesis due to the high degree of collinearity between anatomically defined subdivisions. We demonstrated significantly greater orthogonality in our connectivity-based approach allowing, for the first time to our knowledge, subdivision specific relationships to be investigated. This is illustrated by the fact that several symptom-subdivision relationships were significantly different from each other when examining connectivity defined subdivisions, but no significant differences were observed when examining anatomically defined subdivisions. The greater orthogonality observed with the connectivity-based approach is a natural consequence of the variance induced by the integration of the rs-fMRI data. We demonstrated, however, that this does not come at the expense of significantly reduced reliability. In the case of an anatomical parcellation one may expect a greater number of voxels within a subdivision to increase reliability, and this is supported by the fact that the largest subdivision (associative striatum) shows the greatest reliability. This, however, is not the case for the connectivity-based approach. In the connectivity-based approach, for each subdivision the entire striatum is sampled. Although the sum of fractional weights for a given connectivity defined subdivision might appear to be analogous to the total number of voxels in an anatomical defined subdivision, this is not the case and does not show the same relationship with reliability. For example, if one considers a toy example in which each voxel in a connectivity-based subdivision has the same identical weighting of $<<1$, here the subdivision will possess a low sum of fractional weights, yet its reliability will be equivalent to the entire striatum using an anatomical approach. Indeed, this is one potential reason why greater orthogonality may occur without costing reliability.

In contrast to our connectivity-based approach, traditional anatomically defined subdivisions do not take into account the likely considerable spatial variability in striatal functional specificity that occurs between participants. A connectivity-based approach may be able to account for some of the wide variety that is apparent in terms of striatal volume, shape, and connectivity (48, 49). There are likely, however, both advantages and disadvantages to this approach when one considers that schizophrenia is associated with altered functional corticostriatal connectivity (9), and the fact that both corticostriatal (50), and corticocortical connectivity (36), appear to show a relationship with striatal dopamine function. The optimal approach is therefore likely to depend on the scientific question of interest.

The default mode network predominantly mapped onto striatal areas that have been defined as 'associative' based on their connection to cortical regions broadly involved in cognition (30). Dopamine dysfunction within this region showed an association with the severity of negative/cognitive symptoms. Recent work including both preclinical studies (51, 52), and computational modelling (53) has illustrated how excessive dopamine signalling within the striatum may underlie negative and cognitive symptoms, via a range of mechanisms including impairments in probabilistic learning and disruptions of corticostriatal communication (9). The fact that antipsychotics are relatively ineffective in the treatment of negative symptoms, is consistent with these models as although dopamine antagonism reduces aberrant signalling it also reduces adaptive signalling, thereby potentially exacerbating negative symptoms (54). While it can be hard to determine in first episode cohorts whether negative symptoms are secondary to positive symptoms, the Marder factors we used mitigate against this by maximising the orthogonality of symptom clusters. Previous PET studies have been inconsistent in their findings regarding the relationship between striatal dopamine and negative symptoms. A large proportion of previous DOPA PET studies have not reported the relationship with negative symptoms(45, 55–60), and those that have, often involve low sample sizes and only state that statistical significance was not observed (61–64). Of those that have reported correlation coefficients, a study by Nozaki et al.(65) (n=18) found a statistically non-significant positive relationship between striatal dopamine synthesis capacity and negative symptoms similar to current finding, while a study by Hietala et al.(66) (n=10) reported a non-significant negative relationship. Studies using challenge or depletion paradigms are also inconsistent. One PET study using a depletion paradigm found a relationship between greater negative symptom severity and reduced synaptic dopamine levels in the ventral striatum but did not correct for the multiple subdivisions investigated (25), while another study using the same methods found no significant relationship with synaptic dopamine levels within the whole striatum (67). Differences with the current study may result from marked differences in experimental technique, and the fact that the current study included only first episode patients while the cohort displaying the negative relationship mostly consisted of chronically ill patients. However, given the exploratory nature of these analyses, we suggest the current findings warrant further testing in new cohorts.

As reported previously, we did not observe a significant difference between patients and controls in terms of striatal Ki^{cer} (35). This may represent a type II error, likely exacerbated by the fact that our cohort included a number individuals that were nonresponsive to antipsychotic treatment, a characteristic associated with normal Ki^{cer} (34, 45), and indeed when excluding non-responders there were significant group differences in Ki^{cer} for the DMN and DAT subdivisions.

Future work would benefit from more detailed behavioural assessment, and larger sample sizes would help reduce the risk of both type I and type II error. Reliability studies would ideally use test-retest MRI and PET scans from the same individuals as our approach may have underestimated the reliability of the connectivity-based method. Only 8 individuals contributed to the PET test-retest data, and as such the generalisability of these findings may be limited, however if reliability was found to be lower in a larger data set there is no reason to assume that this would have greater impact on the connectivity-based method compared to an anatomical parcellation. Obtaining PET and MRI measures simultaneously with combined PET-MR may improve the

signal-to-noise ratio. Further work establishing reliability is required and it would be of interest to explore alternative methods for parcellating the striatum, both using resting state data (28, 68), but also mapping anatomical connectivity using diffusion tensor imaging (69), which might show greater stability. It should be noted that a large number of nodes were assigned to the default mode network, including several that would potentially have been assigned to the frontoparietal network if a different community detection algorithm had been employed. There is no single optimal method for either node definition or community assignment, yet different approaches are likely to have a marked impact on results, potentially limiting the generalisability of our findings (70). The reliability of the striatal subdivision defined on the basis of DAT connectivity was poor and alternative methods of defining striatal connectivity on an individual basis may lead to improvements here.

In conclusion, we demonstrate a novel method for generating individualised striatal parcellations and demonstrate some advantages over existing methods, although further validation in future studies is necessary. We show that dopamine synthesis capacity was particularly aberrant within regions of the striatum linked to the default mode network, and that dopamine dysfunction here was strongly associated with the severity of negative symptoms.

Acknowledgments

Funding

RM's work is supported by a clinical research training fellowship grant from the Wellcome trust (no. 200102/Z/15/Z) and by the National Institute for Health Research (NIHR). ODH received funding from Medical Research Council grant MC-A656-5QD30, Maudsley Charity grant 666, support from the US Brain & Behavior Research Foundation, and Wellcome Trust grant 094849/Z/10/Z. MN is a pre-doctoral fellow of the International Max Planck Research School on Computational Methods in Psychiatry and Ageing Research (IMPRS COMP2PSYCH). The participating institutions are the Max Planck Institute for Human Development, Berlin, Germany, and University College London, London, UK. For more information, see: https://www.mps-ucl-centre.mpg.de/en/comp2psych. ODH and MV are supported by the National Institute for Health Research Biomedical Research Centre at South London and Maudsley National Health Service Foundation Trust and King's College London. Data were provided [in part] by the Human Connectome Project, WU-Minn Consortium (Principal Investigators: David Van Essen and Kamil Ugurbil; 1U54MH091657) funded by the 16 NIH Institutes and Centers that support the NIH Blueprint for Neuroscience Research; and by the McDonnell Center for Systems Neuroscience at Washington University.

Competing interests

ODH has received investigator-initiated research funding from and/or participated in advisory/ speaker meetings organised by Astra-Zeneca, Autifony, BMS, Eli Lilly, Heptares, Jansenn, Lundbeck, Lyden-Delta, Otsuka, Servier, Sunovion, Rand and Roche. Neither Dr Howes or his family have been employed by or have holdings/ a financial stake in any biomedical company. M.M. has consulted for Cambridge Cognition, Lundbeck and Forum Pharmaceuticals in the past 3 years. He has also received research funding from Takeda, Eli Lilly and Roche. The other authors report no biomedical financial interests or potential conflicts of interest.

References

1. Arndt S (1995): A Longitudinal Study of Symptom Dimensions in Schizophrenia. *Arch Gen Psychiatry*. 52: 352.
2. McGrath JA, Nestadt G, Liang KY, Lasseter VK, Wolyniec PS, Fallin MD, *et al.* (2004): Five latent factors underlying schizophrenia: Analysis and relationship to illnesses in relatives. *Schizophr Bull*. 30: 855–873.
3. Marder SR, Davis JM, Chouinard G (1997): The effects of risperidone on the five dimensions of schizophrenia derived by factor analysis: combined results of the North American trials. *J Clin Psychiatry*. 58: 538–46.
4. Jauhar S, Krishnadas R, Nour MM, Cunningham-owens D, Johnstone EC, Lawrie SM (2018): Is there a symptomatic distinction between the affective psychoses and schizophrenia ? A machine learning approach. *Schizophr Res*. 202: 241–247.
5. McCutcheon RA, Reis Marques T, Howes OD (2020): Schizophrenia—An Overview. *JAMA Psychiatry*. 77: 201.
6. McTeague LM, Huemer J, Carreon DM, Jiang Y, Eickhoff SB, Etkin A (2017): Identification of common neural circuit disruptions in cognitive control across psychiatric disorders. *Am J Psychiatry*. 174: 676–685.
7. Insel TR, Cuthbert BN (2015): Brain disorders? Precisely. *Science (80-)*. 348: 499–500.
8. Insel T, Cuthbert B, Garvey M, Heinssen R, Pine DS, Quinn K, *et al.* (2010): Research Domain Criteria (RDoC): Toward a new classification framework for research on mental disorders. *Am J Psychiatry*. 167: 748–751.
9. McCutcheon RA, Abi-dargham A, Howes OD (2019): Schizophrenia, Dopamine and the Striatum: From Biology to Symptoms. *Trends Neurosci*. (1-12).
10. Heinz A, Schlagenhauf F (2010): Dopaminergic dysfunction in schizophrenia: salience attribution revisited. *Schizophr Bull*. 36: 472–485.
11. Laruelle M, Abi-dargham A (1999): Dopamine as the wind of the psychotic ¢ re : new evidence from brain imaging studies. 13: 358–371.
12. Laruelle M, Abi-Dargham a, Gil R, Kegeles L, Innis R (1999): Increased dopamine transmission in schizophrenia: relationship to illness phases. *Biol Psychiatry*. 46: 56–72.
13. Abi-Dargham a, Gil R, Krystal J, Baldwin RM, Seibyl JP, Bowers M, *et al.* (1998): Increased striatal dopamine transmission in schizophrenia: confirmation in a second cohort. *Am J Psychiatry*. 155: 761–7.
14. Jauhar S, Nour MM, Veronese M, Rogdaki M, Bonoldi I, Azis M, *et al.* (2017): A test of the transdiagnostic dopamine hypothesis of psychosis using positron emission tomographic imaging in bipolar affective disorder and schizophrenia. *JAMA Psychiatry*. 74: 1206–1213.
15. Simpson EH, Kellendonk C (2017): Insights About Striatal Circuit Function and Schizophrenia From a Mouse Model of Dopamine D2Receptor Upregulation. *Biol Psychiatry*. 81: 21–30.
16. Gold JM, Waltz JA, Matveeva TM, Kasanova Z, Strauss GP, Herbener ES, *et al.* (2012): Negative symptoms in schizophrenia result from a failure to represent the expected value of rewards: Behavioral and computational modeling evidence HHS Public Access. *Arch Gen Psychiatry*. 69: 129–138.
17. McCutcheon RA, Krystal JH, Howes OD (2020): Dopamine and glutamate in schizophrenia: biology,

symptoms and treatment. *World Psychiatry*. 19: 15–33.

18. Haber SN (2016): Corticostriatal circuitry. *Dialogues Clin Neurosci*. 18: 7–21.
19. Phillips ML, Drevets WC, Rauch SL, Lane R (2003): Neurobiology of Emotion Perception I : The Neural Basis of Normal Emotion Perception. . doi: 10.1016/S0006-3223(03)00168-9.
20. Guo L, Walker WI, Ponvert ND, Penix PL, Jaramillo S (2018): Stable representation of sounds in the posterior striatum during flexible auditory decisions. *Nat Commun*. 9: 1534.
21. Grahn JA, Parkinson JA, Owen AM (2008): Progress in Neurobiology The cognitive functions of the caudate nucleus. 86: 141–155.
22. McGuire PK, Bates JF, Goldman-Rakic PS (1991): Interhemispheric integration: II. Symmetry and convergence of the corticostriatal projections of the left and the right principal sulcus (PS) and the left and the right supplementary motor area (SMA) of the rhesus monkey. *Cereb Cortex*. 1: 408–417.
23. Frank MJ, O'Reilly RC (2006): A mechanistic account of striatal dopamine function in human cognition: Psychopharmacological studies with cabergoline and haloperidol. *Behav Neurosci*. 120: 497–517.
24. Howes OD, Montgomery AJ, Asselin MC, Murray RM, Valli I, Tabraham P, *et al.* (2009): Elevated striatal dopamine function linked to prodromal signs of schizophrenia. *Arch Gen Psychiatry*. 66: 13.
25. Kegeles LS, Abi-Dargham A, Frankle WG, Gil R, Cooper TB, Slifstein M, *et al.* (2010): Increased synaptic dopamine function in associative regions of the striatum in schizophrenia. *Arch Gen Psychiatry*. 67: 231–9.
26. McCutcheon R, Beck K, Jauhar S, Howes OD (2018): Defining the Locus of Dopaminergic Dysfunction in Schizophrenia: A Meta-analysis and Test of the Mesolimbic Hypothesis. *Schizophr Bull*. 44: 1301–1311.
27. Choi EY, Yeo BTT, Buckner RL (2012): The organization of the human striatum estimated by intrinsic functional connectivity. *J Neurophysiol*. 108: 2242–2263.
28. Jaspers E, Balsters JH, Kassraian Fard P, Mantini D, Wenderoth N (2017): Corticostriatal connectivity fingerprints: Probability maps based on resting-state functional connectivity. *Hum Brain Mapp*. 38: 1478–1491.
29. Mawlawi O, Martinez D, Slifstein M, Broft A, Chatterjee R, Hwang D, *et al.* (2001): Imaging Human Mesolimbic Dopamine Transmission With Positron Emission Tomography : I . Accuracy and Precision of D 2 Receptor Parameter Measurements in Ventral Striatum. *J Cereb Blood Flow Metab*. 21: 1034–1057.
30. Martinez D, Slifstein M, Broft A, Mawlawi O, Hwang D, Huang Y, *et al.* (2003): Imaging Human Mesolimbic Dopamine Transmission With Positron Emission Tomography . Part II : Amphetamine-Induced Dopamine Release in the Functional Subdivisions of the Striatum. *J Cereb Blood Flow Metab*. 23: 285–300.
31. Egerton A, Demjaha A, McGuire P, Mehta MA, Howes OD (2010): The test-retest reliability of 18F-DOPA PET in assessing striatal and extrastriatal presynaptic dopaminergic function. *Neuroimage*. 50: 524–531.
32. Van Essen DC, Smith SM, Barch DM, Behrens TEJ, Yacoub E, Ugurbil K (2013): The WU-Minn Human Connectome Project: An overview. *Neuroimage*. 80: 62–79.
33. World Health Organization (1992): *The ICD-10 classification of mental and behavioural disorders*. .
34. Jauhar S, Veronese M, Nour MM, Rogdaki M, Hathway P, Turkheimer FE, *et al.* (2018): Determinants of treatment response in first-episode psychosis: an 18F-DOPA PET study. *Mol Psychiatry*. . doi: 10.1038/s41380-018-0042-4.

35. Jauhar S, McCutcheon R, Borgan F, Veronese M, Nour MM, Pepper F, *et al.* (2018): The relationship between cortical glutamate and striatal dopamine function in first episode psychosis: a multi-modal PET and MRS imaging study. *Lancet Psychiatry*. 5: 816–823.

36. McCutcheon R, Nour MM, Dahoun T, Jauhar S, Pepper F, Expert P, *et al.* (2018): Mesolimbic Dopamine Function is Related to Salience Network Connectivity: An Integrative PET and MR Study. *Biol Psychiatry*. 1–11.

37. Kumakura Y, Cumming P (2009): PET Studies of Cerebral Levodopa Metabolism: A Review of Clinical Findings and Modeling Approaches. *Neurosci*. 15: 635–650.

38. Turkheimer FE, Aston JAD, Asselin M-C, Hinz R (2006): Multi-resolution Bayesian regression in PET dynamic studies using wavelets. *Neuroimage*. 32: 111–121.

39. Gordon EM, Laumann TO, Adeyemo B, Huckins JF, Kelley WM, Petersen SE (2016): Generation and Evaluation of a Cortical Area Parcellation from Resting-State Correlations. *Cereb Cortex*. 26: 288–303.

40. Blondel VD, Guillaume JL, Lambiotte R, Lefebvre E (2008): Fast unfolding of communities in large networks. *J Stat Mech Theory Exp*. 2008: 1–12.

41. Parent A, Hazrati L (1995): Functional anatomy of the basal ganglia. I. THe cortico-basal ganglia-thalamo-cortical loop. *Brain Res Rev*. 20: 91–127.

42. Gamer M, Lemon J, Singh P (2019): irr: Various Coefficients of Interrater Reliability and Agreement. .

43. Shrout PE, Fleiss JL (1979): <Shrout1979.pdf>. 86: 420–428.

44. Silver NC, Hittner JB, May K (2004): Testing dependent correlations with nonoverlapping variables: A monte carlo simulation. *J Exp Educ*. 73: 53–69.

45. Demjaha A, Murray RM, McGuire PK, Kapur S, Howes OD (2012): Dopamine synthesis capacity in patients with treatment-resistant schizophrenia. *Am J Psychiatry*. 169: 1203–10.

46. Society RS (2016): Controlling the False Discovery Rate : A Practical and Powerful Approach to Multiple Testing Author (s): Yoav Benjamini and Yosef Hochberg Source : Journal of the Royal Statistical Society . Series B (Methodological), Vol . 57 , No . 1 Published by : . 57: 289–300.

47. Cicchetti D V (1993): Guidelines , Criteria , and Rules of Thumb for Evaluating Normed and. *Psychol Assess*. 6: 284–290.

48. Levitt JJ, Nestor PG, Levin L, Pelavin P, Lin P, Kubicki M, *et al.* (2017): Reduced Structural Connectivity in Frontostriatal White Matter Tracts in the Associative Loop in Schizophrenia. *Am J Psychiatry*. 174: 1102–1111.

49. Chakravarty MM, Rapoport JL, Giedd JN, Raznahan A, Shaw P, Collins DL, Lerch JP (2015): Striatal Shape Abnormalities as Novel Neurodevelopmental Endophenotypes in Schizophrenia : A Longitudinal Study. 1469: 1458–1469.

50. Kim S, Jung WH, Howes OD, Veronese M, Turkheimer FE, Lee Y, *et al.* (2018): Frontostriatal functional connectivity and striatal dopamine synthesis capacity in schizophrenia in terms of antipsychotic responsiveness : an [18 F] DOPA PET and fMRI study. .

51. Simpson EH, Kellendonk C, Kandel E (2010): A possible role for the striatum in the pathogenesis of the cognitive symptoms of schizophrenia. *Neuron*. 65: 585–96.

52. Simpson EH, Kellendonk C (2016): Insights about Striatal Circuit Function and Schizophrenia from a Mouse Model of D2 Receptor Upregulation. *Biol Psychiatry*. 1–10.

53. Maia T V., Frank MJ (2016): An Integrative Perspective on the Role of Dopamine in Schizophrenia. *Biol Psychiatry*. 1–15.

54. Maia T V., Frank MJ (2017): An Integrative Perspective on the Role of Dopamine in Schizophrenia. *Biol Psychiatry*. 81: 52–66.

55. Reith J, Benkelfat C, Sherwin a, Yasuhara Y, Kuwabara H, Andermann F, *et al.* (1994): Elevated dopa decarboxylase activity in living brain of patients with psychosis. *Proc Natl Acad Sci U S A*. 91: 11651–4.

56. Lindstrom LH, Gefvert O, Hagberg G, Lundberg T (1999): Increased dopamine synthesis rate in medial prefrontal cortex and striatum in schizophrenia indicated by L-(- 11 C) DOPA and PET. *Biol Psychiatry*. 46: 681–688.

57. Elkashef A, Doudet D, Bryant T (2000): 6- 18 F-DOPA PET study in patients with schizophrenia. *Psychiatry Res Neuroimaging*. 100: 1–11.

58. Meyer-Lindenberg A, Miletich RS, Kohn PD, Esposito G, Carson RE, Quarantelli M, *et al.* (2002): Reduced prefrontal activity predicts exaggerated striatal dopaminergic function in schizophrenia. *Nat Neurosci*. 5: 267–71.

59. Shotbolt P, Stokes PR, Owens SF, Toulopoulou T, Picchioni MM, Bose SK, *et al.* (2011): Striatal dopamine synthesis capacity in twins discordant for schizophrenia. *Psychol Med*. 41: 2331–8.

60. Kim E, Howes OD, Veronese M, Beck K, Seo S, Park JW, *et al.* (2017): Presynaptic Dopamine Capacity in Patients with Treatment-Resistant Schizophrenia Taking Clozapine: An [18F]DOPA PET Study. *Neuropsychopharmacology*. 42: 941–950.

61. Dao-Castellana MH, Paillère-Martinot ML, Hantraye P, Attar-Lévy D, Rémy P, Crouzel C, *et al.* (1997): Presynaptic dopaminergic function in the striatum of schizophrenic patients. *Schizophr Res*. 23: 167–74.

62. Hietala J, Syvälahti E, Kuoppamäki M, Hietala J, Syvälahti E, Haaparanta M, *et al.* (1995): Presynaptic dopamine function in striatum of neuroleptic-naive schizophrenic patients. *Lancet*. 346: 1130–1131.

63. Kumakura Y, Cumming P, Vernaleken I, Buchholz H-G, Siessmeier T, Heinz A, *et al.* (2007): Elevated [18F]fluorodopamine turnover in brain of patients with schizophrenia: an [18F]fluorodopa/positron emission tomography study. *J Neurosci*. 27: 8080–7.

64. Howes OD, Williams M, Ibrahim K, Leung G, Egerton A, McGuire PK, Turkheimer F (2013): Midbrain dopamine function in schizophrenia and depression: a post-mortem and positron emission tomographic imaging study. *Brain*. 136: 3242–3251.

65. Nozaki S, Kato M, Takano H, Ito H, Takahashi H, Arakawa R, *et al.* (2009): Regional dopamine synthesis in patients with schizophrenia using L-[beta-11C]DOPA PET. *Schizophr Res*. 108: 78–84.

66. Hietala J, Syvälahti E, Vilkman H, Vuorio K, Räkköläinen V, Bergman J, *et al.* (1999): Depressive symptoms and presynaptic dopamine function in neuroleptic-naive schizophrenia. *Schizophr Res*. 35: 41–50.

67. Abi-dargham A, Rodenhiser J, Printz D, Zea-ponce Y, Gil R, Kegeles LS, *et al.* (2000): Increased baseline occupancy of D2 receptors by dopamine in schizophrenia. *Proc Natl Acad Sci U S A*. 97: 8104–8109.

68. Barnes (2010): Identifying basal ganglia divisions in individuals using resting-state functional connectivity MRI. *Front Syst Neurosci*. 4: 1–10.

69. Tziortzi AC, Searle GE, Tzimopoulou S, Salinas C, Beaver JD, Jenkinson M, *et al.* (2011): Imaging dopamine receptors in humans with [11C]-(+)-PHNO: Dissection of D3 signal and anatomy. *Neuroimage*.

54: 264–277.

70. Zalesky A, Fornito A, Harding IH, Cocchi L, Yücel M, Pantelis C, Bullmore ET (2010): Whole-brain anatomical networks: Does the choice of nodes matter? *Neuroimage*. 50: 970–983.

Variable	*Controls (N=21)*	*Patients (N=29)*	*p*
Male, n (%)	13(62%)	22(76%)	0.45[2]
Age, years mean (SD)	23.3(3.4)	25.5(4.2)	0.06[3]
Ethnicity, white British, n (%)	14(67%)	10(35%)	0.05[2]
Current smoker, n (%)	5(24%)	12(41%)	0.32[2]
Right handed, n (%)	19(90%)	26(90%)	0.99[2]
Years in education, mean (SD)	16.8(1.9)	14.2(3.4)	0.002[3]
Medication status, n (%) Antipsychotic naïve Minimally treated[1] Antipsychotic free	 NA NA NA	 11(38%) 2(7%) 16(55%)	NA
Diagnosis, n (%) Schizophrenia Bipolar Other	 NA NA NA	 15 (52) 12 (41) 2(7)	NA
Days between PET and MRI scans (median, IQR, range)	70 (24-250, 4-733)	8 (3-24, 1-371)	<0.001[4]
PANSS Total, mean (SD) PANSS Positive, mean (SD) PANSS Negative, mean (SD) PANSS General, mean (SD)	NA NA NA NA	66.7(20.7) 17.6(6.9) 15.1(6.3) 34.0(10.1)	NA
Injected Activity, MBq mean (SD)	152.9(12.6)	143.5(7.4)	0.01[3]

Table 1 Demographic details of study participants

Data are expressed as n (%) or mean (SD). PANSS=Positive and Negative Syndrome Scale.

[1]Receiving antipsychotic medication for 2 weeks or less

2Chi-square test

[3]Independent sample t-test

[4]Kruskal-Wallis test

Subdivision	*Controls (N=21)*	*Patients (N=29)*	*Responders (N=11)*	*P value (control-patient) degrees freedom =48*	*P value (control-responder) degrees freedom=30*
Whole striatum	1.29(0.11)	1.28(0.10)	1.34(0.08)	0.78	0.16
Associative striatum	1.29(0.11)	1.288(0.10)	1.35(0.088)	0.73	0.14
Limbic Striatum	1.29(0.12)	1.26(0.10)	1.31(0.08)	0.45	0.54
Sensorimotor Striatum	1.30(0.14)	1.30(0.10)	1.35(0.10)	0.98	0.20
AUD	1.22(0.15)	1.21(0.18)	1.20(0.18)	0.27	0.85
CON	1.33(0.20)	1.20(0.14)	1.36(0.15)	0.61	0.66
DAT	1.22(0.18)	1.28(0.15)	1.34(0.15)	0.24	0.028
DMN	1.12(0.16)	1.17(0.16)	1.25(0.09)	0.27	0.009
SMN	1.28(0.15)	1.24(0.15)	1.27(0.13)	0.30	0.75

p values calculated using an independent sample t-test

Table 2
Patient-control comparisons for subdivision Ki^{cer} values

Figure 1 Overview of methods

(i) Participants receive resting state MRI and ^{18}F-DOPA PET scans (A) Cortical nodes are assigned to networks based on corticocortical resting state functional connectivity (B) Connectivity of each striatal voxel to these cortical networks is calculated (C) Weighted striatal connectivity maps produced for each network (see Figure S2) (D) Voxelwise Ki^{cer} maps weighted by these striatal connectivity maps to give a Ki^{cer} value for each network

(ii) Significance testing of Ki^{cer}-symptom relationships using a permutation testing approach. In addition to permuting at the level of participants (not pictured) cortical ROIs were permuted to generate null distributions: (A) Cortical ROIs shuffled into random networks 10,000 times (B) These shuffled network sets used to calculate Ki^{cer} with the same method described above in (i) (C) Symptom-Ki^{cer} correlations calculated for each null set of Ki^{cer} (D) Null distribution created from repeating step C for each of the null network sets (E) True symptom-Ki^{cer} correlation values compared to null distribution to test statistical significance.

AUD- Auditory , CON – Cinguloperсular, DAT – Dorsal attention, DMN – Default mode, SMN – Sensorimotor.

Figure 2. Connectivity defined striatal maps

Striatal connectivity maps used to weight voxelwise Ki^{cer} maps and generate network specific Ki^{cer}s. Group averaged maps are shown while individualised maps were used in practice. Maps are normalised by total connectivity strength. Greater intensity of colour indicates that a voxel displays greater connectivity to the cortical network in question. In order to show differences between networks more clearly thresholded maps are also shown (retaining only top 35% of voxels). The anatomically defined Martinez parcellation is also shown in the bottom right.

AUD- Auditory , CON – Cinguloperсular, DAT – Dorsal attention, DMN – Default mode, SMN – Sensorimotor.

Figure 3 Comparison of connectivity defined and anatomically defined subdivisions

A) Heatmap displaying correlation coefficients between Ki^{cer} values for different subdivisions. There is greater orthogonality between connectivity defined subdivisions(AUD, DAT,CON,SMN,DMN) (r_p = 0.23-0.67) compared to anatomically defined (LST, AST, SMST)(r_p=0.71-0.91)

B) Comparing the magnitude of these intra-method correlation coefficients, these are significantly lower (*= $p<0.05$) for the connectivity-based method (i.e indicating greater orthogonality) for all but 5 of the 30 comparisons.

Anatomically defined subdivisions: AST – Associative Striatum, LST – Limbic Striatum, SMST – Sensorimotor striatum
Connectivity defined subdivisions: AUD- Auditory , CON – Cinguloperсular, DAT – Dorsal attention, DMN – Default mode, SMN – Sensorimotor

Figure 4. Relationships between dopamine synthesis capacity and psychotic symptoms

A) Associations between PANSS Marder factors and striatal Ki^{cer} across different striatal subdivisions regions. Heatmap displays r_p values. Statistical significance calculated by permuting participants. (*=$p<0.05$, **=$p<0.05$ FDR corrected)

B) The strongest association observed using the connectivity-based approach was between DMN-Ki^{cer} and the Marder negative factor score (r_p=0.49, p=0.009).

C) Heatmaps illustrating the extent to which symptom-Ki associations differ between subdivisions. Positive values indicate that the row subdivision shows a greater association with the Marder factor than the column subdivision (*=$p<0.05$).

Connectivity defined subdivisions: AUD- Auditory , CON – Cinguloperсular, DAT – Dorsal attention, DMN – Default mode, SMN – Sensorimotor.
Anatomcially defined subdivisions: WST – Whole striatum, AST – Associative Striatum, LST – Limbic Striatum, SMST – Sensorimotor striatum

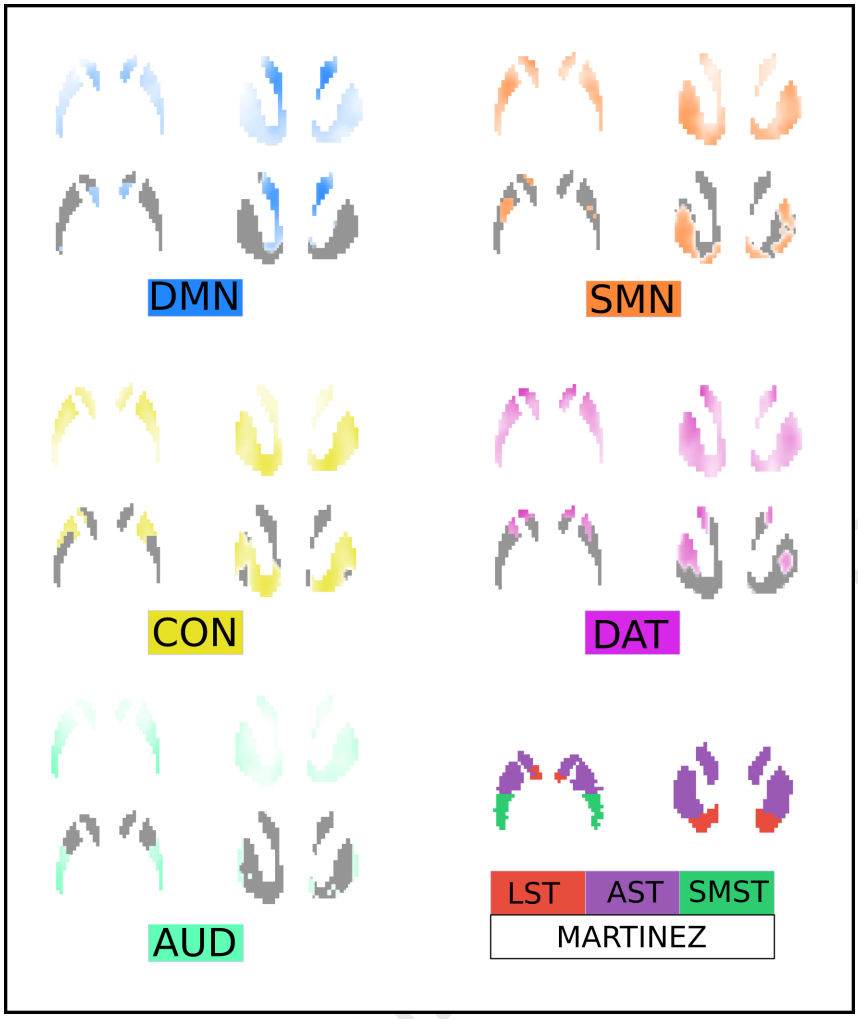

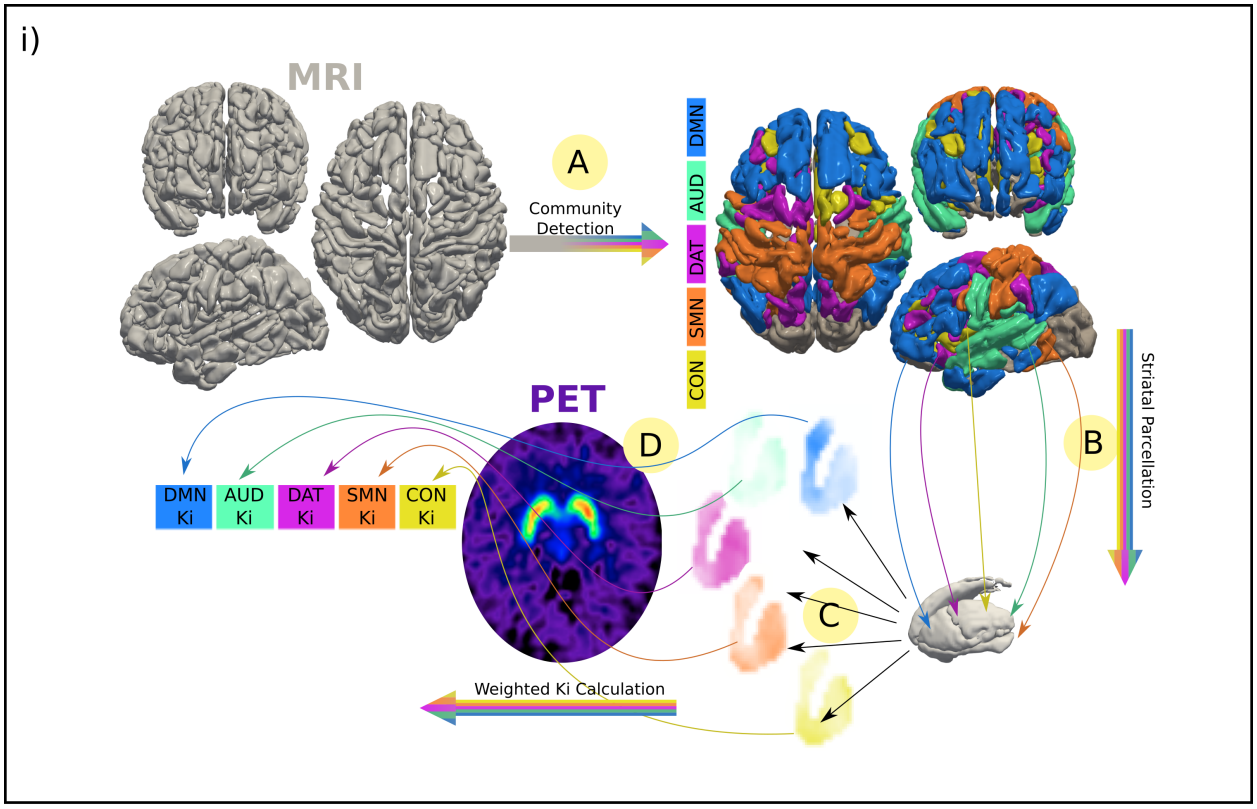
i)
MRI
A
Community Detection
DMN
AUD
DAT
SMN
CON
PET
D
B
Striatal Parcellation
DMN Ki
AUD Ki
DAT Ki
SMN Ki
CON Ki
C
Weighted Ki Calculation

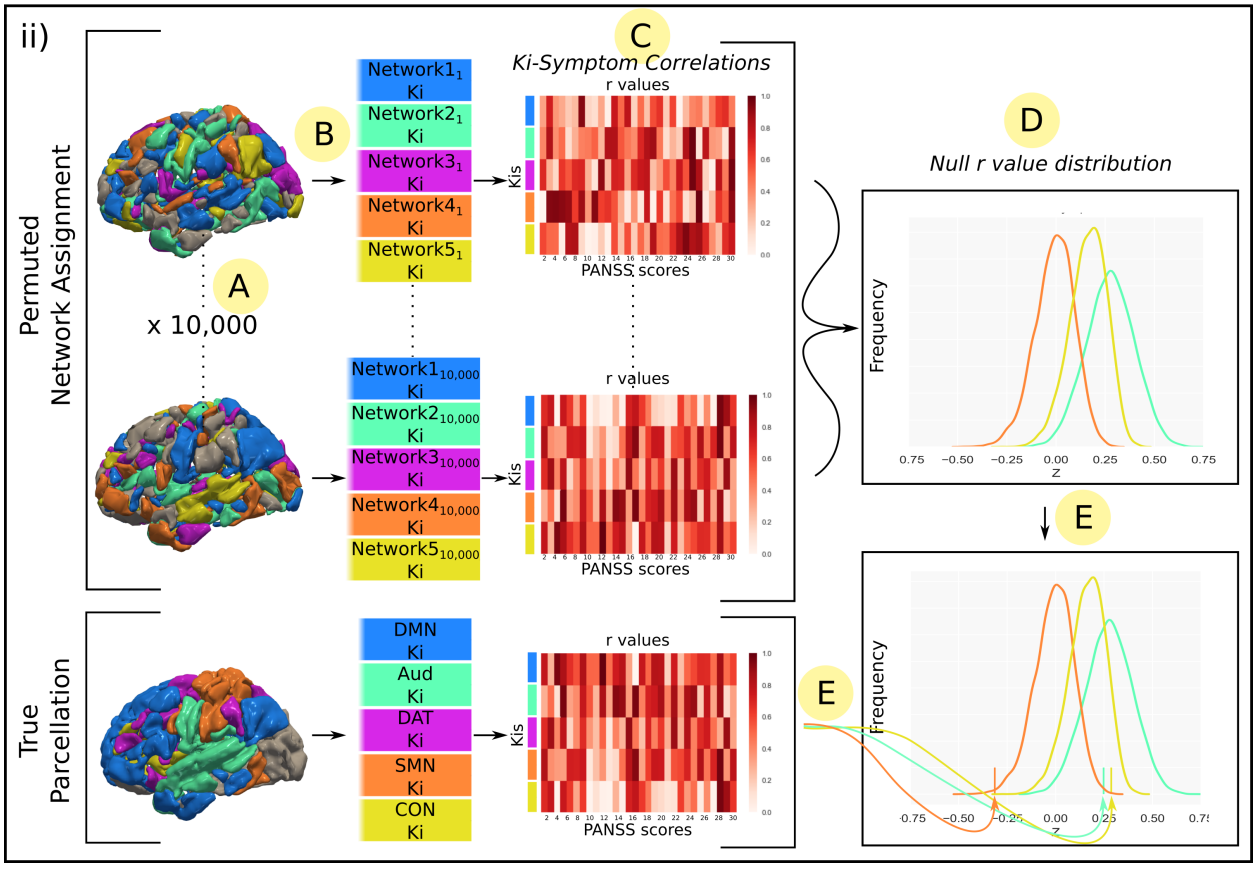
ii)
Permuted Network Assignment
A
x 10,000
B
C
Ki-Symptom Correlations
r values
PANSS scores
Kis
D
Null r value distribution
Frequency
z
E
True Parcellation

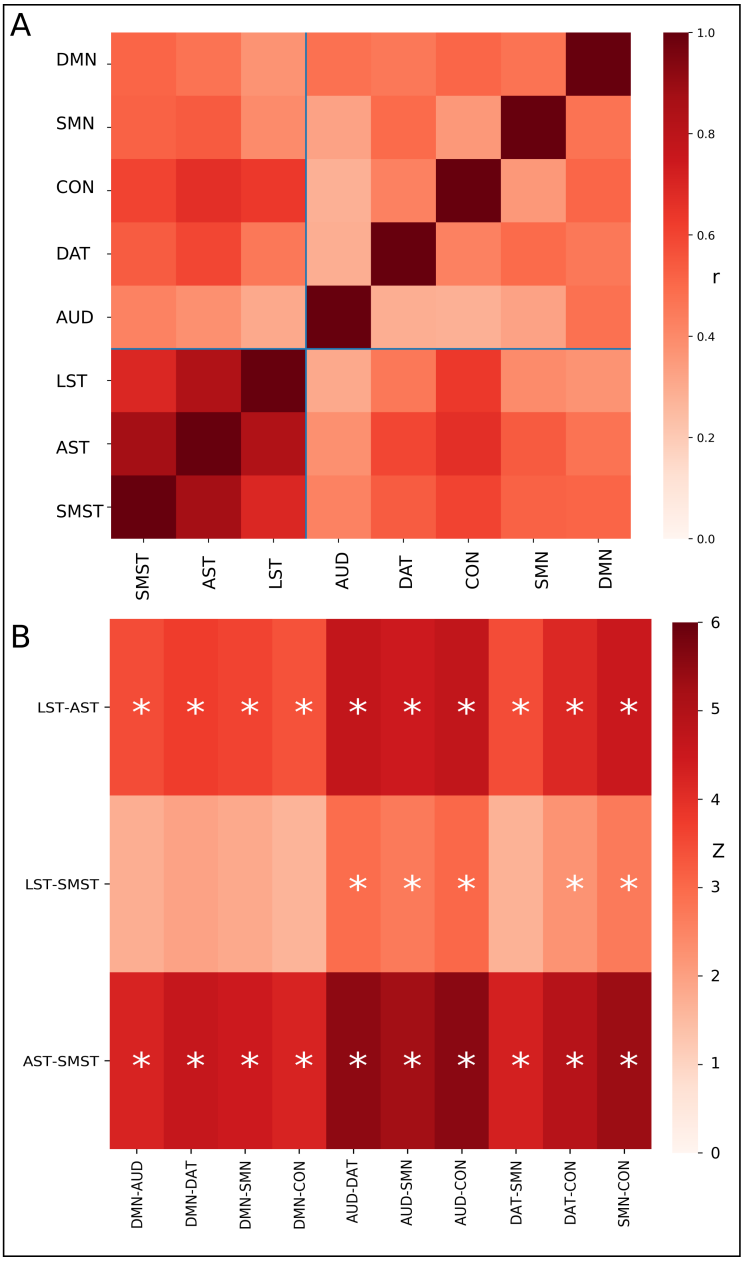
A
DMN
SMN
CON
DAT
AUD
LST
AST
SMST
SMST
AST
LST
AUD
DAT
CON
SMN
DMN
1.0
0.8
0.6
0.4
0.2
0.0
r
B
LST-AST
LST-SMST
AST-SMST
DMN-AUD
DMN-DAT
DMN-SMN
DMN-CON
AUD-DAT
AUD-SMN
AUD-CON
DAT-SMN
DAT-CON
SMN-CON
6
5
4
3
2
1
0
Z

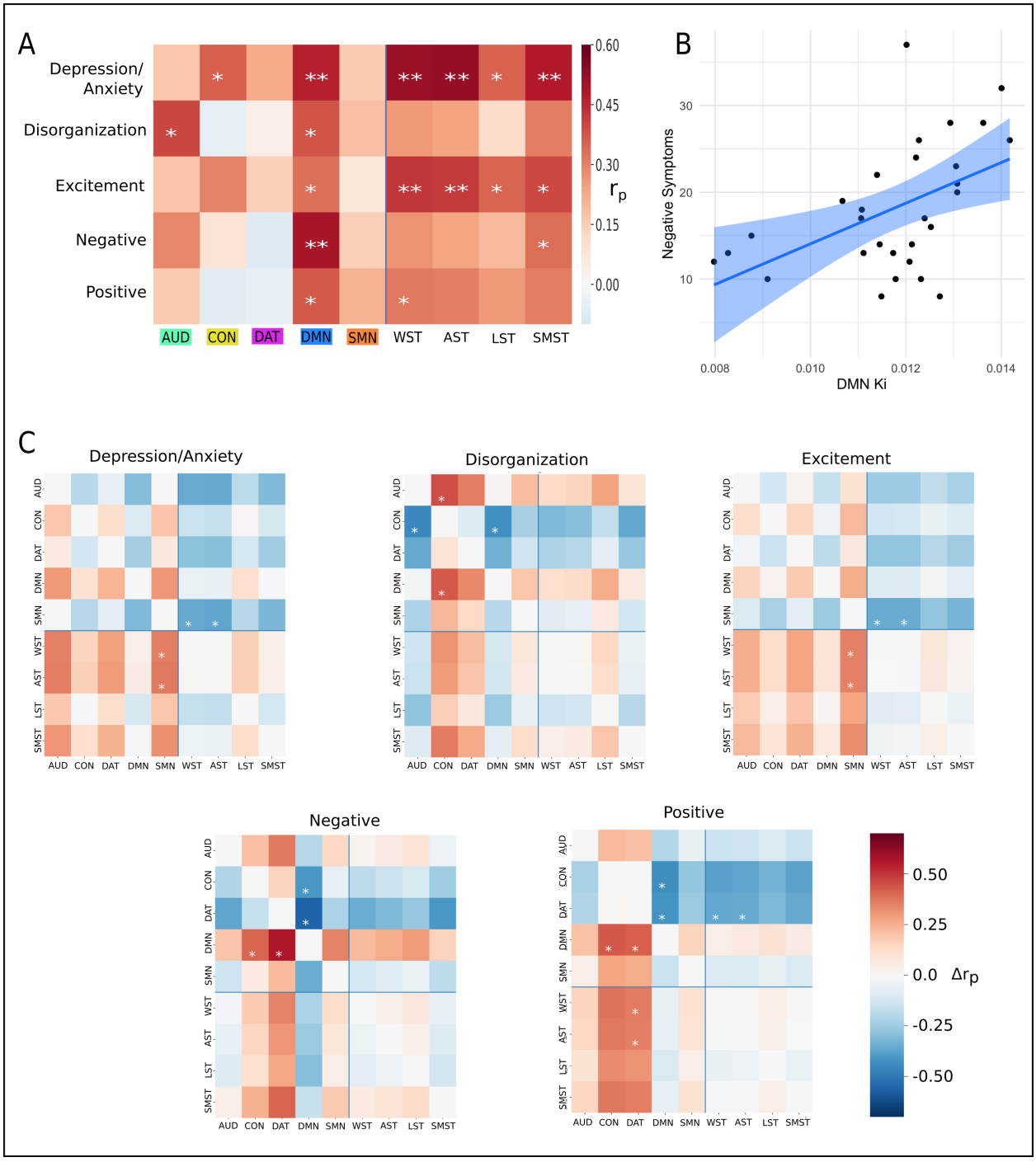
A
Depression/ Anxiety
Disorganization
Excitement
Negative
Positive
AUD CON DAT DMN SMN WST AST LST SMST
0.60
0.45
0.30
0.15
0.00
r_p
B
Negative Symptoms
DMN Ki
0.008 0.010 0.012 0.014
10 20 30
C
Depression/Anxiety
Disorganization
Excitement
Negative
Positive
0.50
0.25
0.0
-0.25
-0.50
Δr_p